Multi-UAV Trajectory Control, Resource Allocation, and NOMA User Pairing for Uplink Energy Minimization

Minh Tri Nguyen, *Student Member, IEEE*, and Long Bao Le, *Senior Member, IEEE*

***Abstract*—In this work, we study the joint optimization of multiple unmanned aerial vehicles (UAVs)' trajectories, power allocation, user-UAV association, and user pairing for UAV-assisted wireless networks employing the nonorthogonal multiple access (NOMA) for uplink communications. The design aims to minimize the total energy consumption of ground users while guaranteeing to successfully transmit their required amount of data to the UAV-mounted base stations. The underlying problem is a mixed-integer nonlinear program (MINLP), which is difficult to solve optimally. To tackle this problem, we derive the optimal power allocation as a function of other variables, which is used to transform the optimization problem into an equivalent form. We then propose an iterative algorithm to solve the resulting optimization problem by using the block coordinate descent (BCD) method where three subproblems are solved in each iteration and this process is repeated until convergence. Specifically, given the UAVs' trajectories and data rates, we solve the NOMA user pairing, and user-UAV association subproblem optimally by exploiting its special structure. Then, we describe how to optimize the users' data rates and tackle the UAV trajectory optimization in the second and third subproblems, respectively, by using the successive convex approximation (SCA) method. Numerical results show that our proposed algorithm can provide efficient active-inactive schedules (by setting user's transmit powers to zero), and lower energy consumption compared to an existing baseline, and an OMA-based resource allocation and UAV-trajectory optimization strategy.**

***Index Terms*—Nonorthogonal multiple access (NOMA) user pairing, resource allocation, unmanned aerial vehicle (UAV), UAV trajectory optimization.**

I. Introduction

UNMANNED aerial vehicles (UAVs) have been emerging as one of the key components of future wireless networks, thanks to their mobility, flexibility, and adaptive altitude [1]. In particular, the performance of UAV-based wireless networks in terms of coverage, throughput, and energy efficiency can be significantly enhanced by properly controlling UAVs' trajectories leveraging the potential Line-of-Sight (LoS) communications between UAVs and ground users [2]. In general, UAV communications can be employed to enhance the communications of existing terrestrial communications infrastructure and support various applications, such as military, surveillance, monitoring, and data collection for Internet of Things (IoT) [3]. The Internet of drones (or UAVs) has been one major research area in the broad area of IoT where drones play the role of communications things. Moreover, UAV communication is expected to play an important role in 5G and beyond-5G wireless systems [4].

From the connectivity viewpoint, the world has witnessed the rapidly increasing number of IoT connections to support many emerging applications in recent years [5]. The design of energy-efficient IoT wireless networks is critical to elongate working durations of IoT devices and wireless networks [6]. There have been growing interests in leveraging UAV communications to enable energy-efficient operations (e.g., data collection and data dissemination) of IoT wireless networks [7]–[9]. In particular, efficient placement or trajectory control of UAVs and resource allocation can lead to reliable/LoS communications between IoT devices and UAVs enhancing their energy efficiency.

From the resource allocation perspective, nonorthogonal multiple access (NOMA) can significantly improve the spectral efficiency by allowing multiple users to communicate using the same time/frequency/space resources [10]. In the uplink NOMA, users with different channel conditions transmit their data simultaneously using the same frequency band and different transmit power levels. At the receiver, the received signals are decoded in sequence by using the successive interference cancelation (SIC) technique. The employment of NOMA in the UAV-based wireless networks enables to leverage the advantages of both NOMA and UAV communications. In this direction, the works [9], [11]–[13] address different design problems for NOMA-enabled UAV-based wireless networks where UAVs' placement/trajectories are jointly optimized with other network functions. In particular, the work [9] minimizes the UAV's flight time for data collection where NOMA-based user scheduling, transmit power allocation, and UAVs' locations are optimized. Duan *et al.* [11] and Zhang *et al.* [12] investigated the resource allocation problems that aim to maximize the system throughput of UAV-based wireless networks in the uplink and downlink communications scenarios, respectively. Furthermore, maximization of the minimum achievable rate of ground users in the downlink NOMA communications is studied in [13] through the

Manuscript received 10 December 2021; revised 22 June 2022; accepted 30 June 2022. Date of publication 6 July 2022; date of current version 21 November 2022. This work was supported in part by the Innovation for Defence Excellence and Security (IDEaS) Program from the Department of National Defence (DND) under Grant MN3-005. *(Corresponding author: Long Bao Le.)*

The authors are with INRS, Université du Québec, Montréal, QC H5A 1K6, Canada (e-mail: minh.tri.nguyen@inrs.ca; long.le@inrs.ca).

Digital Object Identifier 10.1109/JIOT.2022.3188867

joint optimization of UAV trajectory, transmit power, and user association.

Optimization of energy efficiency and power consumption in NOMA-enabled wireless networks have also been studied in several existing works [14]–[16] where it has been shown that NOMA is indeed more energy efficient than the conventional orthogonal multiple access (OMA) in [17]. More recently, energy/power optimization for NOMA-enabled UAV-based wireless networks has been addressed in [18]–[20]. Specifically, the work [18] considers the minimization of total energy consumption of ground users by optimizing the NOMA user pairing and single UAV's trajectory for uplink communications using NOMA. Shi *et al.* [19] studied the power minimization problem for the single-UAV wireless network serving multiple users while ensuring their required Quality of Service (QoS). An energy minimization problem is considered in [20] for the multi-UAV setting where each user communicates with all UAVs simultaneously using different channels with fixed bandwidth. This design may activate some non-LoS communications links, which reduces the achievable spectral efficiency. Moreover, all users are clustered into a single NOMA group, which considerably increases the complexity and decreases the reliability of the SIC process [21]. Nevertheless, most previous works either consider NOMA user pairing and placement of multiple static UAVs [11], [19], [22]–[26] or joint NOMA user pairing and single-UAV trajectory optimization [9], [18], [27], [28] . However, the joint optimization of NOMA user pairing and multi-UAV trajectories could result in much better performance for UAV-based networks, which has not been studied in the current literature.

In terms of problem formulation and solution approaches, the designs of NOMA-enabled UAV-based wireless networks usually involve solving mixed-integer nonlinear problems (MINLPs) ([9], [11], [12], [18], [19], [23], [26]–[29], to name a few). In these papers, the underlying MINLPs are tackled by using different methods, including noniterative multistep algorithms [9], [11], [18], [19], [23], [26], [29], and iterative block coordinate descent (BCD) (for minimization problems) or block coordinate ascent (BCA) for maximization problems [12], [27], [28]. In BCD or BCA algorithms, the variable set is decomposed into smaller subsets (e.g., power variables and UAV trajectory control variables) and optimization of one subset of variables given the values of other variables in the corresponding subproblem is performed sequentially in each iteration and this process is repeated until convergence. It is worth mentioning that the BCD-based approach is more numerically efficient when the value of the objective function is improved over iterations. This can be observed from numerical studies in [12], [27], and [28] where throughput-related objective functions are considered. However, the BCD-based approach cannot be directly applied to solve the energy/power optimization problem where the objective function contains only power optimization variables. This is because subproblems optimizing variables other than power variables are simply feasibility checking problems and solving feasibility checking problems does not improve the overall objective function over iterations. Therefore, further analysis and problem transformations are required before the BCD approach can be applied to solve power/energy minimization problems.

Two notable observations can be drawn from the above literature survey. First, to the best of our knowledge, the joint optimization of NOMA user pairing, resource allocation, and multi-UAV trajectory control has not been studied in the literature. Second, using the BCD-based approach to solve energy minimization problems in NOMA-enabled UAV-based wireless networks is nontrivial because of the special structure of these underlying optimization problem as discussed above. Our current work aims to fill these gaps in the literature where we make the following key contributions.

1) We formulate the total energy minimization problem where NOMA user pairing, transmit power allocation, user-UAV association, and multi-UAV trajectory control are jointly optimized. Our design ensures that users can successfully transmit their required amount of data to the UAVs in the uplink direction. We derive the optimal power allocation solution, which is expressed explicitly as a function of other optimization variables. Substituting this optimal power allocation into the objective function enables us to achieve an equivalent optimization problem for which we can employ the BCD method to solve the underlying problem.
2) We develop an efficient algorithm, called multi-UAV NOMA energy minimization (MUNE), to solve the considered problem by using the BCD approach. Specifically, we solve three smaller subproblems iteratively until convergence. The first problem optimizes user pairing and user-UAV association, given UAVs' trajectories, and data rates in each time slot, where we transform this subproblem into several maximum weighted matching problems (MWMP) whose solutions can be found in polynomial time [30]. The second subproblem optimizes the user data rate in each time slot while the third problem optimizes the UAVs' trajectories given the values of other optimization variables. We employ the successive convex approximation (SCA) method to convexity and solve these two subproblems efficiently.
3) To evaluate the performance of the proposed algorithm, we compare it with two other baselines. The first baseline is the data collection optimization algorithm (DCOA), which was developed in [18]. The second baseline is called the multi-UAV OMA energy minimization (MUOE) algorithm, which employs the same design principles as for our proposed MUNE algorithm; however, the conventional OMA instead of NOMA is used in MUOE. We show the convergence of the proposed MUNE algorithm, its typical achieved UAVs' trajectories, and the superior performance of our algorithm compared to the two considered baselines via numerical studies. Moreover, we demonstrate the tradeoff between the UAV flight time and the total energy as well as the impacts of different parameters such as the numbers of users and UAVs on the total energy consumption.

The remainder of this article is organized as follows. The system model and problem formulation are presented in

TABLE I
LIST OF NOTATIONS

Notations	Explanation
N	Number of UAVs
K	Number of users
T	Number of time slots
δ	Length of one time slot
E_{all}	Total energy consumption of all users in the service period
B	Channel bandwidth assigned for each NOMA user pair
D_k	Data transmission demand of user k
h	Altitude of UAVs
μ	Channel power gain at reference distance
σ^2	Power of white Gaussian noise
$\mathbf{u}_k$	2-D coordinate of user k
$\mathbf{c}_n[t]$	2-D coordinate of UAV n in time slot t
$\mathbf{c}_{\mathsf{o}}$	2-D coordinate of UAV launching station
$\mathbf{D}_{\mathsf{safe}}$	Safe distance for UAVs
$\mathbf{V}_{\mathsf{max}}$	UAV's maximum speed
$p_k[t]$	Transmit power of user k in time slot t
P_{max}	Maximum user transmit power
$a_{k;n}[t]$	Association variable for UAV n and user k in time slot t
$x_{k,l}[t]$	User pairing variable for users k and l in time slot t
$\tau_{k;n}[t]$	Channel power gain for user k and UAV n in time slot t
$\tau_k[t]$	Channel power gain of user k in time slot t
$\lambda_k[t]$	Strong-weak role of user k in its pair in time slot t
$\mathsf{R}_k[t]$	Data rate of user k who is a strong user in time slot t
$\mathsf{r}_k[t]$	Data rate of user k who is a weak user in time slot t
$r_k[t]$	Target data rate of user k in time slot t
$\mathbf{p}[t]$	Collection of all user transmit powers in time slot t
$\mathbf{A}[t]$	Collection of user-UAV association variables in time slot t
$\mathbf{X}[t]$	Collection of user pairing variables in time slot t
$\mathbf{\Lambda}[t]$	Collection of strong-weak role variables in time slot t
$\mathbf{r}[t]$	Collection of target data rates of all users in time slot t

Section II. We describe our proposed algorithm in Section III. Numerical results are presented in Section IV followed by conclusion in Section V.

For notations, we use bold normal letters to denote vectors and bold capitalized letters to denote matrices. If a variable $\mathbf{x}[t]$ has different values for different time slots t, we use $\{\mathbf{x}[t]\}$ to denote the set of all $\mathbf{x}[t], t = 1, \ldots, T$. As for the indices, we use semicolons (;) to separate indices that belong to different categories (i.e., users, UAVs, and time slots) and commas (,) to separate indices that belong to the same category. The indicator function is denoted as $\mathbb{1}_{x>y}$ which takes value 1 when $x > y$ and takes value 0, otherwise. The base-2 logarithm and the natural logarithm of x are denoted as $\log(x)$ and $\ln(x)$, respectively. The summary of key notations used in this article is given in Table I.

II. System Model and Problem Formulation

A. System Model

We consider uplink communications in a UAV-assisted wireless network with N flying UAVs and K ground users. The UAV flying duration is divided into T small time slots, each of which has an identical length of δ. We assume that UAV n flies at the fixed altitude h and its 2-D coordinate at time slot t is denoted as $\mathbf{c}_n[t]$. The 2-D coordinate of ground user k is denoted as $\mathbf{u}_k$. We assume that NOMA is employed to support the uplink communications where users are grouped into two-user pairs, which transmit their data on orthogonal channels. Moreover, it is assumed that each user k requires to transmit an amount of data D_k to the UAVs by the end of the service period.[1] The considered UAV-assisted wireless network is illustrated in Fig. 1.

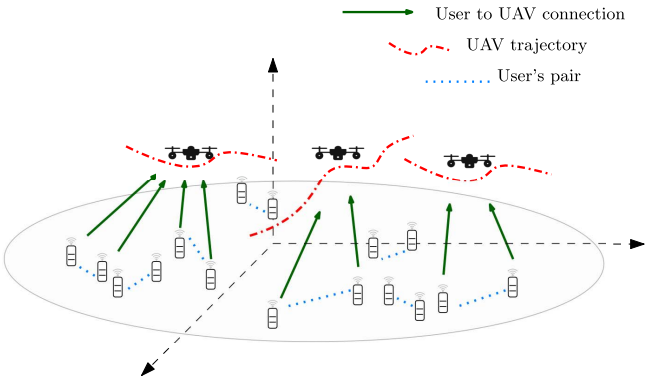

Fig. 1. System model.

The LoS channel is assumed for the communication between users and UAVs. When the UAVs fly sufficiently high, this assumption aligns with the results observed in field tests [2]. In this work, the UAV altitude is assumed to be set appropriately to achieve the desirable LoS communications while it should be low to achieve the strong channels between GUs and UAVs. Furthermore, the channel power gain between user k and UAV n at t, denoted as $\tau_{k;n}[t]$, can be expressed as follows:

$$\tau_{k;n}[t] = \frac{\mu}{\|\mathbf{c}_n[t] - \mathbf{u}_k\|^2 + h^2} \tag{1}$$

where μ is the channel power gain at the reference distance of 1 m from the transmitter. Note that this channel model also aligns with the 3GPP standard for UAV communications [31].

B. User-UAV Association and NOMA User Pairing

Let $a_{k;n}[t]$ represent the association between user k and UAV n in time slot t where $a_{k;n}[t]$ is equal to 1 if user k is associated[2] with UAV n and equal to 0, otherwise. We assume that each user can only connect to one UAV but each UAV can connect to multiple users in any time slot. Therefore, we have the following constraints:

$$\sum_{n=1}^{N} a_{k;n}[t] = 1 \quad \forall k, t. \tag{2}$$

Using the association variables, the channel power gain of user k at t can be expressed as follows:

$$\tau_k[t] = \sum_{n=1}^{N} a_{k;n}[t]\tau_{k;n}[t] \quad \forall k, t. \tag{3}$$

Now, let $x_{k,l}[t]$ denote the user pairing decision variable that is equal to 1 if user k is paired with user l in time slot t and equal to 0, otherwise. We then have $x_{k,l} = 0$ if $k = l$, and $x_{k,l}[t] = x_{l,k}[t]$ for all k and l. In fact, there is a coupling between the user association and user pairing decision

[1] These data transmission demand constraints are typically needed in data collection scenarios for IoT applications.

[2] In this article, "connected" and "associated" are used interchangeably to describe the user-UAV association.

variables. Specifically, if users k and l are paired with each other in time slot t, we should have $a_{k;n}[t] = a_{l;n}[t] \quad \forall n$, i.e., if users k and l are paired with each other, both users k and l must be associated with the same UAV. This coupling constraint can be expressed as follows:

$$x_{k,l}[t]\big(a_{k;n}[t] - a_{l;n}[t]\big) = 0 \quad \forall (k,l), n, t. \tag{4}$$

C. NOMA Uplink Communications

We assume that users are paired and each user pair transmits data to the associated UAV in the uplink direction. The data received by the UAV are then decoded as follows. The message of the user in each pair with the better channel condition (strong user) is decoded first where the signal from the user with worse channel condition (weak user) is considered as noise. After the message of the strong user is decoded and removed from the received signal, the message of the weak user is decoded. Specifically, if user k is the strong user in a particular pair, its achieved data rate in time slot t can be expressed as follows:

$$\mathsf{R}_k[t] = B\log\left(1 + \frac{\tau_k[t]p_k[t]}{\sigma^2 + \tau_k^{\mathsf{p}}[t]p_k^{\mathsf{p}}[t]}\right) \tag{5}$$

where B is the channel bandwidth assigned for the underlying user pair, σ^2 is the power of the Gaussian white noise, $\tau_k[t]$ and $p_k[t]$ are the power gain and transmit power of user k, respectively, and $\tau_k^{\mathsf{p}}[t]$ and $p_k^{\mathsf{p}}[t]$ are the channel power gain and transmit power of its paired user, respectively, which can be expressed as follows:

$$\tau_k^{\mathsf{p}}[t] = \sum_{l=1}^{K} x_{k,l}[t]\tau_l[t] \tag{6a}$$

$$p_k^{\mathsf{p}}[t] = \sum_{l=1}^{K} x_{k,l}[t]p_l[t]. \tag{6b}$$

If user k is the weak user in the considered pair in time slot t, its achieved data rate can be expressed as follows:

$$\mathsf{r}_k[t] = B\log\left(1 + \frac{\tau_k[t]p_k[t]}{\sigma^2}\right). \tag{7}$$

D. Strong-Weak Relation for NOMA User Pairs

We need to capture the strong-weak relation between users in each pair and time slot. Specifically, we use $\lambda_k[t]$ to describe the strong-weak role of user k where it is equal to 1 if user k is the strong user and equal to 0 if it is the weak user in its associated pair and time slot t. Note that a user is strong or weak depending on its channel condition and the channel condition of its partner. In our design, the channel condition of a particular user depends on the coordinates of the associated UAV and the UAVs' coordinates are optimization variables. Therefore, it is necessary to define variables capturing the strong–weak roles of individual users. In fact, strong–weak variables play a crucial role in the problem formulation as will be detailed in the next section.

Alternatively, one could express the strong–weak variables by using indicator functions, i.e., $\lambda_k[t] = \mathbb{1}_{\tau_k[t]>\tau_k^{\mathsf{p}}[t]}$. Moreover, for the special network with a single UAV, one could simply determine the strong-weak channel conditions based on the distances from users to the UAV, without explicitly using $\lambda_k[t]$, as in [9], [18], [27], and [32]. However, it is nontrivial to extend the approach in these works to the multi-UAV-based networks, where the distances between users and their associated UAVs strongly depend on the user associations, which are unknown in advance and need to be optimized.

Furthermore, there is also coupling between the strong–weak variables and the user-pairing optimization variables. Specifically, if user k is paired with user l, only one of them is the strong user. This coupling can be expressed in the following constraints:

$$x_{k,l}[t](\lambda_k[t] + \lambda_l[t] - 1) = 0 \quad \forall (k,l), t. \tag{8}$$

Finally, the relationship between channel conditions and strong-weak variables can be stated as follows:

$$\tau_k[t] \geq \tau_k^{\mathsf{p}}[t], \quad \text{if} \quad \lambda_k[t] = 1 \tag{9a}$$

$$\tau_k[t] \leq \tau_k^{\mathsf{p}}[t], \quad \text{if} \quad \lambda_k[t] = 0. \tag{9b}$$

The inequalities (9a) and (9b) can be expressed by the following inequality:

$$(2\lambda_k[t] - 1)\Big(\tau_k[t] - \tau_k^{\mathsf{p}}[t]\Big) \geq 0 \quad \forall k, t. \tag{10}$$

The definition of strong–weak variables are convenient for the problem formulation; however, strong couplings between them and other variables, captured in (8) and (10), render the optimization problem difficult to solve. In addition, the values of strong–weak variables can be readily determined (as values of the indicator function $\mathbb{1}_{\tau_k[t]>\tau_k^{\mathsf{p}}[t]}$) when the UAV trajectories, user association, and user pairing variables are given. In the following, the strong–weak variables are occasionally omitted if they can be readily determined from the given values of other variables without causing any ambiguity.

E. Problem Formulation

Our design aims to minimize the energy consumption of all users by optimizing the user association ($\mathbf{A}[t]$), user pairing ($\mathbf{X}[t]$), the strong–weak variables ($\mathbf{\Lambda}[t]$), the power allocation ($\mathbf{p}[t]$), and the UAV trajectories $\{\mathbf{c}_n[t]\}$. Additionally, we want to ensure that users be able to transmit their required amount of data to the UAVs within the service duration of T time slots. For our considered scenario, it becomes essential to simply to minimize the energy consumption of ground users (e.g., sensors) to prolong its operation time while imposing the data communication demand constraints. The considered optimization problem can be stated as follows:

$$\mathcal{P}_0: \min_{\{\mathbf{A}[t],\mathbf{X}[t],\mathbf{\Lambda}[t],\mathbf{p}[t],\mathbf{c}_n[t]\}} E_{\mathsf{all}}$$

$$\text{s.t.} \sum_{t=1}^{T} \delta(\lambda_k[t]\mathsf{R}_k[t] + (1-\lambda_k[t])\mathsf{r}_k[t]) \geq D_k \quad \forall k \tag{11a}$$

$$\mathbf{X}[t] = \mathbf{X}^T[t] \quad \forall t \tag{11b}$$

$$\sum_{l=1}^{K} x_{k,l}[t] = 1 \quad \forall k, t \tag{11c}$$

$$p_k[t] \le P_{\max} \quad \forall k, t \tag{11d}$$

$$\|\mathbf{c}_n[t] - \mathbf{c}_n[t-1]\| \le \delta V_{\max} \quad \forall n, t \tag{11e}$$

$$\|\mathbf{c}_n[t] - \mathbf{c}_m[t]\| \ge D_{\text{safe}} \quad \forall t \quad \forall n \ne m \tag{11f}$$

$$\mathbf{c}_n[1] = \mathbf{c}_n[T] = \mathbf{c}_0 \quad \forall n \tag{11g}$$

$$\lambda_k \in \{0,1\}, a_{k;n} \in \{0,1\}, x_{k,l} \in \{0,1\} \quad \forall k, l, n$$

$$\text{constraints} \quad (2), (4), (8), (10) \tag{11h}$$

where $P_{\max}$ denotes the maximum transmit power of each user, and the total energy can be expressed as

$$E_{\text{all}} = \delta \sum_{t=1}^{T} \sum_{k=1}^{K} p_k[t]. \tag{12}$$

Constraint (11a) ensure that every user can transmit their required amount of data to the UAVs. Constraints (11b) and (11c) are imposed to make sure that the user pairing solution is valid. Constraint (11d) describes the maximum transmit powers of users. Constraint (11e) captures the maximum distance that a UAV can travel in one time slot, where $V_{\max}$ is the UAV's maximum speed. Constraint (11f) is imposed to avoid collision among UAVs, i.e., interdistance between UAVs must be at least D_{safe} (meters). Constraints (11g) set the initial and final positions of UAVs, where $\mathbf{c}_0$ is the coordinate of the launching station and constraints (11h) define different binary variables.

The formulated problem is an MINLP, which is nontrivial to solve. In the next section, we propose an algorithm to solve problem $\mathcal{P}_0$ efficiently.

III. Proposed Algorithms

A. Equivalent Problem Transformation

First, we introduce a set of auxiliary variables $\{\mathbf{r}[t]\}$, where $r_k[t]$ is the target data rate in time slot t for which user k transmits data to the UAVs to fulfill the data transmission demand. We can transform problem $\mathcal{P}_0$ into the following equivalent problem with additional variables $\{\mathbf{r}[t]\}$:

$$\mathcal{P}_1: \min_{\{\mathbf{A}[t],\mathbf{X}[t],\mathbf{\Lambda}[t],\mathbf{p}[t],\mathbf{c}_n[t],\mathbf{r}[t]\}} E_{\text{all}}$$

$$\text{s.t.} \quad \lambda_k[t]\mathsf{R}_k[t] + (1-\lambda_k[t])\mathsf{r}_k[t] \ge r_k[t] \quad \forall k, t \tag{13a}$$

$$\sum_{k=1}^{K} \delta r_k[t] \ge D_k \quad \forall k$$

$$(2), (4), (8), (10)$$

$$(11b), (11c), (11d), (11e), (11f), (11g), (11h). \tag{13b}$$

The left-hand side of (13a) describes the achievable data rate of user k, which is equal to the rate of a strong user or a weak user depending on the strong–weak role of this user. Constraint (13a) captures the fact that the target rate $r_k[t]$ is upper bounded by the achievable data rate. Moreover, (13b) describes the data transmission demand constraints expressed by using the target data rates. It can easily seen that problems $\mathcal{P}_0$ and $\mathcal{P}_1$ are equivalent [33] and the equality of (13a) holds at optimality. We will describe how to solve problem $\mathcal{P}_1$ in the following. Note that problem $\mathcal{P}_1$ is still an MINLP problem, which is as difficult to solve as problem $\mathcal{P}_0$. However, we will show that the auxiliary variables $\{\mathbf{r}[t]\}$ help us transform problem $\mathcal{P}_1$ into more tractable problems. To this end, we provide an outline of our solution in Section III-B and describe our proposed algorithm in the sections that follows.

B. Outline of Proposed Solution

For the considered optimization problem, we will show that the optimal power $\{\mathbf{p}^*[t]\}$ can be expressed explicitly in terms of other variables ($\{\mathbf{c}_n[t], \mathbf{X}[t], \mathbf{A}[t], \mathbf{r}[t]\}$). This key result will be stated in Lemma 1 in Section III-C. In fact, the derivation of the optimum power $\{\mathbf{p}^*[t]\}$ with respect to other variables enables us to apply the BCD technique to solve problem $\mathcal{P}_1$ effectively.

We then propose to solve problem $\mathcal{P}_1$ by iteratively solving three following subproblems. In the first subproblem, we assume that values of $\{\mathbf{c}_n[t], \mathbf{r}[t]\}$ are given and solve for the optimal power allocation where all other variables are the optimization variables. In the second subproblem, we optimize the data rate variables $\{\mathbf{r}[t]\}$ given $\{\mathbf{c}_n[t]\}$ and the values of other variables obtained from solving the first subproblem. Finally, in the third subproblem, the UAVs' trajectories are optimized given the values of other variables. It can be shown that the total energy consumption is reduced over iterations, hence, the iterative process is guaranteed to converge.

C. Optimizations of Power and Integer Variables Given UAVs' Trajectories and Rates

Assuming that $\{\mathbf{c}_n[t], \mathbf{r}[t]\}$ are given, we develop an algorithm to find the optimal power $\{\mathbf{p}^*[t]\}$ with respect to $\{\mathbf{c}_n[t], \mathbf{r}[t]\}$, and other integer variables. Specifically, we solve for the optimal power and user association when the user pairing solution is known in Section III-C1. Then, the user pairing optimization is solved in Section III-C2 by tackling the underlying maximum weighted graph matching problem. Then, the optimal user association is derived.

1) Optimization Problems as User Pairing Solution Is Given: If the values of $\{\mathbf{c}_n[t], \mathbf{r}[t]\}$, and $\mathbf{X}[t]$ are given, the problem $\mathcal{P}_1$ is reduced to the following problem:

$$\mathcal{P}_{\mathsf{A},\mathsf{P}}: \min_{\mathbf{A}[t]\mathbf{\Lambda}[t],\mathbf{p}[t]} E_{\text{all}}$$

$$\text{s.t.} \quad (2), (4), (8), (10), (11d), (11h), (13a).$$

Furthermore, problem $\mathcal{P}_{\mathsf{A},\mathsf{P}}$ can be decomposed into several subproblems, denoted as $\tilde{\mathcal{P}}_{\mathsf{A},\mathsf{P}}(k, l; t)$ where subproblem $\tilde{\mathcal{P}}_{\mathsf{A},\mathsf{P}}(k, l; t)$ minimizes the total energy consumed by users k and l in time slot t, where the transmit power $p_k[t], p_l[t]$, the user association $\mathbf{a}_k[t], \mathbf{a}_l[t]$, and the strong–weak variables $\lambda_k[t], \lambda_l[t]$ are optimized.[3] This subproblem can be expressed as follows:

$$\tilde{\mathcal{P}}_{\mathsf{A},\mathsf{P}}(k, l; t): \min_{\{\mathbf{a}_i[t],\lambda_i[t],p_i[t]\}_{i=k,l}} \delta(p_k[t] + p_l[t])$$

$$\text{s.t.} \quad a_{k;n}[t] = a_{l;n}[t] \tag{14a}$$

[3]Note that $\mathbf{a}_k[t] = [a_{k;1}[t], \ldots, a_{k;N}[t]]$ denotes the user association vector corresponding to user k at t.

$$\lambda_k[t] + \lambda_l[t] = 1 \tag{14b}$$
$$(2\lambda_k[t] - 1)(\tau_k[t] - \tau_l[t]) \geq 0 \tag{14c}$$
$$(2),\ (11d),\ (11h),\ (13a)$$

where (14a)–(14c) are deduced from (4), (8), and (10), respectively, given that $x_{k,l}[t] = 1$.

Let $p_{k,l}[t]$ denote the sum power of two users k and l in the objective function of $\tilde{\mathcal{P}}_{\mathsf{A,P}}(k, l; t)$, then the total energy consumption can be expressed as follows:

$$E_{\mathsf{all}} = \frac{\delta}{2} \sum_{t=1}^{T} \sum_{k=1}^{K} \sum_{l=1}^{K} x_{k,l}[t] p_{k,l}[t]. \tag{15}$$

In the following, we find the optimal value of $p_{k,l}[t]$ for all t and all combinations of k and l. Specifically, we find the optimal power allocation with respect to the user association variables (i.e., if $\mathbf{a}_k[t]$ and $\mathbf{a}_l[t]$ are known). Note that when the user association solution is given, the channel conditions for k and l are determined by (3). Then, the values of strong-weak variables can also be readily determined by (14b) and (14c).[4] We substitute the optimal power allocation solution as a function of the user association variables into the objective function of $\tilde{\mathcal{P}}_{\mathsf{A,P}}(k, l; t)$ from which the optimal user association solutions with respect to every user pair (k, l) will be determined.

a) Finding optimal power allocation given user association: Let us consider a particular pair of users k and l associated with UAV n. Assume that the channel of user k is stronger than that of user l (i.e., $\lambda_k[t] = 1$ and $\lambda_l[t] = 0$). Then, the problem $\tilde{\mathcal{P}}_{\mathsf{A,P}}(k, l; t)$ can be deduced further into the following problem:

$$\tilde{\mathcal{P}}_{\mathsf{P}}(k, l; t; n): \min_{\{p_i[t]\}_{i=k,l}} \ \delta(p_k[t] + p_l[t]) \quad \text{s.t.} \ (11d),\ (13a).$$

We now state the optimal power allocation in the following lemma.

Lemma 1: If the problem $\tilde{\mathcal{P}}_{\mathsf{P}}(k, l; t; n)$ is feasible, its optimal solution can be stated as follows:

$$p_k^*[t] = \sigma^2 \tau_{k;n}^{-1}[t]\left(\beta^{r_k[t]} - 1\right)\beta^{r_l[t]}$$
$$p_l^*[t] = \sigma^2 \tau_{l;n}^{-1}[t]\left(\beta^{r_l[t]} - 1\right) \tag{16}$$

where $\beta = 2^{1/B}$. Moreover, the problem is feasible if both $p_k^*[t]$ and $p_l^*[t]$ in (16) are no greater than P_{max}.

Proof: The power allocation solution can be derived by using the following steps. First, we equivalently transform constraints (13a) into linear constraints with respect to $p_l[t]$ and $p_k[t]$. The equivalent problem is linear; hence, it is straightforward to derive the minimum required transmit powers for each user. ∎

Note that the results for the downlink case, and when $r_k[t] = r_l[t]$, were stated or can be deduced implicitly in some previous works [15]–[17], [26]. The results in Lemma 1 allow us to explicitly express the optimal transmit powers of users k and l in terms of their channel conditions, which further depend on the user association and distances from the users to their associated UAV. Therefore, hereafter, we will use the right-hand side of (16) instead of $p_k[t]$ and $p_l[t]$.

Let $p_{k,l;n}[t]$ be the optimal allocated power of users k and l assuming that they are paired and connected to UAV n in time slot t. Then, $p_{k,l;n}[t]$ can be expressed as follows:[5]

$$p_{k,l;n}[t] = \begin{cases} \sigma^2\left(\tau_{k;n}^{-1}[t]\left(\beta^{r_k[t]} - 1\right)\beta^{r_l[t]} + \tau_{l;n}^{-1}[t](\beta^{r_l[t]} - 1)\right) \\ \qquad \text{if } \max\left(p_k^*[t], p_l^*[t]\right) \leq P_{\mathsf{max}} \\ \infty, \qquad \text{otherwise.} \end{cases} \tag{17}$$

b) Finding optimal user association: The optimal value of the sum power of users k and l can be expressed with respect to the user association variables as follows:

$$p_{k,l}[t] = \sum_{n=1}^{N} a_{k;n}[t] p_{k,l;n}[t]. \tag{18}$$

Note that (18) is realized with the assumption that $x_{k,l}[t] = 1$, and hence, $a_{k;n}[t] = a_{l;n}[t]$. The result in (18) allows us to find the optimal association for users k and l as stated in the following lemma.

Lemma 2: If $x_{k,l}[t] = 1$, the optimal association for users k and l at t can be found as follows:

$$a_{k;n}^*[t] = a_{l;n}^*[t] = \begin{cases} 1, & \text{if } n = \arg\min_{n} p_{k,l;n}[t] \\ 0, & \text{otherwise.} \end{cases} \tag{19}$$

Substituting the user association solution obtained from Lemma 2, we can find the optimal value of $p_{k,l}[t]$ from (18).

2) User Pairing Optimization Problem: Upon obtaining the optimal user association and the corresponding power allocation solution, the user pairing optimization problem can be expressed as follows:

$$\mathcal{P}_{\mathsf{X}}: \min_{\mathbf{X}[t]} \frac{\delta}{2} \sum_{t=1}^{T} \sum_{k=1}^{K} \sum_{l=1}^{K} x_{k,l}[t] p_{k,l}[t]$$
$$\text{s.t.} \ (11b),\ (11c),\ (11h).$$

Similarly, problem $\mathcal{P}_{\mathsf{X}}$ can be further decomposed into several subproblems each of which optimizes the user pairing for one particular time slot t. These integer linear program subproblems in each time slot t is indeed the maximum weight perfect matching (MWPM) problem for a graph whose vertices are users, and the weight of the edge between users k and l is $p_{k,l}[t]$. This MWPM problem can be solved efficiently and optimally by using different algorithms, such as Edmon's algorithm [30] and Galil's algorithm [34]. Interested readers are encouraged to read [35] for detailed discussions of different algorithms to solve various classes of graph matching problems. Note that Edmon's algorithm has been used to solve the NOMA user pairing problem in [36].

In the following sections, we describe how to tackle the optimizations of other variables, given user association and user pairing solutions. We denote $(k, l)[t]$ as the users k and l

[4] Specifically, if users k and l are associated with UAV n in time slot t, we can compute their channel conditions according to (1). Then, $\lambda_k[t] = 1$ if $\tau_{k;n}[t] \geq \tau_{l;n}[t]$ and $\lambda_l[t] = 0$, otherwise.

[5] We use the convention in [33] where the optimal value of a minimization problem is infinity if the problem is infeasible.

to be paired in time slot t. Without loss of generality, it is the convention in the following sections that k is the strong user and l is the weak user.

D. Data Rate Optimization

From (12) and (17), the total energy consumption E_{all} can be expressed with respect to the data rates $\{\mathbf{r}[t]\}$ as follows:

$$E_{\mathsf{all}} = \delta\sigma^2 \sum_{t=1}^{T} \sum_{(k,l)[t]} \beta^{r_k[t]+r_l[t]} \tau_k^{-1}[t] + \beta^{r_l[t]} \left(\tau_l^{-1}[t] - \tau_k^{-1}[t]\right) - \delta\sigma^2 \sum_{t=1}^{T} \sum_{(k,l)[t]} \tau_l^{-1}[t]. \tag{20}$$

Note that the term in the second line is a constant, which does not depend on $\{\mathbf{r}[t]\}$. When UAV trajectory, user association, and user pairing solutions are given, the optimization of data rates can be stated as follows:

$$\mathcal{P}_{\mathsf{R}}: \min_{\{\mathbf{r}[t]\}} E_{\mathsf{all}}$$

$$\text{s.t.} \sum_{k=1}^{K} \delta r_k[t] \geq D_k \quad \forall k \tag{21a}$$

$$\beta^{r_l[t]} - 1 \leq \frac{P_{\mathsf{max}}}{\sigma^2} \tau_k[t] \quad \forall (k,l)[t], \tag{21b}$$

$$\beta^{r_k[t]+r_l[t]} - \beta^{r_l[t]} \leq \frac{P_{\mathsf{max}}}{\sigma^2} \tau_l[t] \quad \forall (k,l)[t]. \tag{21c}$$

Since $\tau_l^{-1}[t] - \tau_k^{-1}[t] \geq 0$ for all user pairs $(k,l)[t]$, the objective function of problem $\mathcal{P}_{\mathsf{R}}$ is convex; however, problem $\mathcal{P}_{\mathsf{R}}$ is still nonconvex due to the nonconvexity of constraint (21c). However, it can be seen that (21c) is the difference of two convex functions; hence, we can approximate (21c) by the following constraint [33]:

$$\beta^{r_k[t]+r_l[t]} - \beta^{\bar{r}_l[t]}(1 + \ln(\beta)(r_l[t] - \bar{r}_l[t]))\tau_{l;n}^{-1}[t] \leq \frac{P_{\mathsf{max}}}{\sigma^2} \tag{22}$$

where we have replaced $\beta^{r_l[t]}$ by its first-order Taylor approximation at local point $\bar{r}_l[t]$. On the left-hand side of (22), the first term is convex and the second term is linear with respect to the optimization variables $(r_k[t], r_l[t])$; hence, (22) is a convex constraint. Therefore, the SCA technique can be applied to solve the problem $\mathcal{P}_{\mathsf{R}}$ iteratively where constraint (21c) is replaced by constraint (22) in each iteration of the iterative process.

E. UAV Trajectory Optimization

Using the results in (1), (12), and (17), the total energy E_{all} can also be expressed as a function of the UAVs' trajectories $\{\mathbf{c}_n[t]\}$ as follows:

$$E_{all} = \delta\sigma^2 \sum_{t=1}^{T} \sum_{(k,l)[t]} \zeta_k[t] \left\|\mathbf{c}_{n_{(k,l)}}[t] - \mathbf{u}_k\right\|^2 + \zeta_l[t] \left\|\mathbf{c}_{n_{(k,l)}}[t] - \mathbf{u}_l\right\|^2 + \delta\sigma^2 \sum_{t=1}^{T} \sum_{(k,l)[t]} (\zeta_k[t] + \zeta_l[t]) h^2 \tag{23}$$

where $\zeta_k[t] = \mu^{-1}(\beta^{r_k[t]} - 1)\beta^{r_l[t]}$ and $\zeta_l[t] = \mu^{-1}(\beta^{r_l[t]} - 1)$; $\mathbf{c}_{n_{(k,l)}}[t]$ is the coordinate of the UAV serving user pair $(k,l)[t]$. Note that the second term does not depend on $\{\mathbf{c}_n[t]\}$.

The UAV trajectory optimization problem can be expressed as follows:

$$\mathcal{P}_{\mathsf{C}}: \min_{\{\mathbf{c}_n[t]\}} E_{\mathsf{all}}$$

$$\text{s.t.} \ \zeta_k[t] \left(\left\|\mathbf{c}_{n_{(k,l)}}[t] - \mathbf{u}_k\right\|^2 + h^2 \right) \leq \frac{P_{\mathsf{max}}}{\sigma^2} \quad \forall (k,l)[t] \tag{24a}$$

$$\zeta_l[t] \left(\left\|\mathbf{c}_{n_{(k,l)}}[t] - \mathbf{u}_l\right\|^2 + h^2 \right) \leq \frac{P_{\mathsf{max}}}{\sigma^2} \quad \forall (k,l)[t]$$

$$(10), (11e), (11g), (11f). \tag{24b}$$

Even though problem $\mathcal{P}_{\mathsf{C}}$ is nonconvex due to the nonconvex constraint (11f), we can solve it by applying the SCA method. Specifically, we first square both sides of (11f) and then approximate the left-hand side with its lower bound at the local point $\{\bar{\mathbf{c}}_n[t], \bar{\mathbf{c}}_m[t]\}$ by using the first-order Taylor expansion. We then can obtain the following approximated constraint:

$$2(\bar{\mathbf{c}}_m[t] - \bar{\mathbf{c}}_n[t])^T (\mathbf{c}_m[t] - \mathbf{c}_n[t]) - \|\bar{\mathbf{c}}_m[t] - \bar{\mathbf{c}}_n[t]\|^2 \geq D_{\mathsf{safe}}^2. \tag{25}$$

As constraints (11f) are approximated by (25), the resulting approximated problem of problem $\mathcal{P}_{\mathsf{C}}$ is convex with respect to the UAV trajectory variables. Therefore, the obtained convex problem can be solved optimally using standard solvers.

F. Proposed Algorithm

Our proposed iterative algorithm, named MUNE, is described in Algorithm 1. In this algorithm, ϵ is a small positive number that is set to balance between the desired accuracy and convergence time of this algorithm. Note that ϵ is also used and set to control the convergence speed of SCA algorithms applied to solve problems $\mathcal{P}_{\mathsf{R}}$ and $\mathcal{P}_{\mathsf{C}}$.

G. Convergence and Complexity Analysis

Solving each problem $\mathcal{P}_{\mathsf{A,P}}$, $\mathcal{P}_{\mathsf{R}}$, and $\mathcal{P}_{\mathsf{C}}$ iteratively results in a sequence of nondecreasing numbers corresponding to the values of the underlying objective function where the power variables are substituted by the function of other variables according to (16). In other words, the value of the objective function will increase over iterations to reach the convergence point. Note that the achieved solution at convergence is optimal for the power, NOMA user pairing, and user association variables, and is locally optimal for the UAV trajectory variables.

In this work, all optimization problems are solved by using the CVX solver, which employs the interior-point method with the complexity of $\mathcal{O}(\kappa^{1/2}(\kappa + \upsilon)\upsilon^2)$, where κ is the number of inequality constraints and υ is the number of variables [37]. We assume that the number of UAVs N is small compared to the number of users K as in most practical scenarios. Then, the complexity involved in solving problems $\mathcal{P}_{\mathsf{A,P}}$, $\mathcal{P}_{\mathsf{R}}$, and $\mathcal{P}_{\mathsf{C}}$ are $\mathcal{O}(TK^4)$, $\mathcal{O}(T^3K^3)$, and $\mathcal{O}(T^{1.5} \times \max(K^{1.5}, T^{1.5}))$, respectively. Therefore, the overall complexity of Algorithm 1 is $\mathcal{O}(K^3(K + T^2)T)$.

Algorithm 1 MUNE

1: Initiate values for UAV trajectories $\{\mathbf{c}_n^0[t], \mathbf{r}^0[t]\}$, set $i = 1$, $E_{\text{all}}^0 = TKP_{\max}$.
2: **while** 1 **do**
3: Given $\{\mathbf{c}_n^{i-1}[t], \mathbf{r}^{i-1}[t]\}$, solve problem $\tilde{\mathcal{P}}_{\mathsf{A,P}}(k, l; t)$ for all t and all possible user pairs (k, l), obtain optimal $\{p_{k,l}[t]\}$ from (18).
4: From the obtained $\{p_{k,l}[t]\}$, solve problem $\mathcal{P}_{\mathsf{X}}$ for optimal user pairing variables $\{\mathbf{X}^i[t]\}$, and the corresponding user association variables $\{\mathbf{A}^i[t]\}$.
5: Solve problem $\mathcal{P}_{\mathsf{R}}$ given the values of other variables iteratively until convergence, obtain the values of $\{\mathbf{r}^i[t]\}$.
6: Solve problem $\mathcal{P}_{\mathsf{C}}$ given the values of other variables iteratively until convergence. Let $\{\mathbf{c}_n^i[t]\}$ and E_{all}^i denote the obtained UAVs' trajectories and the corresponding total energy consumption, respectively.
7: **if** $E_{\text{all}}^{i-1} - E_{\text{all}}^i \leq \epsilon$ **then**
8: Break the loop.
9: **else**
10: Let $i = i + 1$.
11: **end if**
12: **end while**
13: End of algorithm.

H. Baseline Algorithms

We now introduce two baseline algorithms whose performances will be compared with that achieved by our proposed algorithm in the next section.

The first baseline algorithm, called DCOA, was developed in [18], in which the generalized benders decomposition [38] is used to solve the joint NOMA user pairing and power allocation optimization problem. Then, the UAV trajectory is optimized to maximize the total transmitted data from all users. The key idea is that when the total transmitted data exceed the required amount of transmitted data, the energy consumption can be reduced by solving the power minimization problem in the next iteration. The DCOA can only be applied to the single UAV setting.

To demonstrate the importance of nonorthogonal access to the achievable performance, we also present the second baseline algorithm, called MUOE, whose details are given in the Appendix, where the OMA strategy is used instead of NOMA. The MUOE algorithm can be applied to single and multi-UAV settings. In this OMA-based strategy, each user is connected to the closest UAV and they have an assigned bandwidth of $B/2$ in each time slot.

IV. Numerical Results

We consider a circular network area with the radius of 1000 m in which users are placed randomly and uniformly. We assume that UAVs fly at the fixed altitude of $h = 100$ m and all users require the same amount of data to be collected $D_k = 6$ Mbits $\forall k$, unless stated otherwise. The bandwidth allocated for each user pair is 100 kHz, the noise power is set to -105 dBm, and μ is set equal to 6.5×10^{-4}. The number of time slots is $T = 60$, unless stated otherwise and each time slot has the length of $\delta = 1$ s. Note that because the locations of GUs are fixed and the adopted channel gains only depend on GU-UAV distances, the optimization can be performed offline. The optimization must only be redone if the number and/or locations of GUs change, which would not occur very frequently. The maximum transmit power is $P_{\max} = 0.1$ W and the value of ϵ in Algorithm 1 controlling the numerical accuracy and convergence time is set at 10^{-2}.

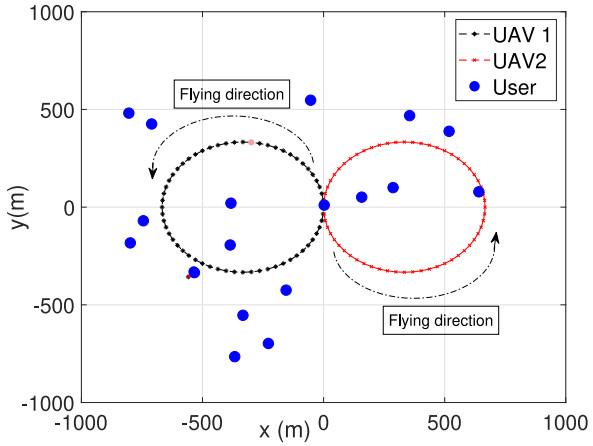

Fig. 2. User's locations and UAV's initial trajectories.

The UAV station is located at the center of the network area, $\mathbf{c}_{\mathsf{O}} = (0, 0)$. Regarding the values of $\{\mathbf{r}^0[t]\}$, we set $r_k^0[t] = D_k/T$ for all user k, i.e., the initial data rates in each time slot are identical for all users. Note that we do not set the initial values for user pairing, user association, and user transmit powers, as they are to be optimized in the first iteration by Algorithm 1. For the UAVs' initial trajectories, we let UAV n start at $\mathbf{c}_{\mathsf{O}} = (0, 0)$ and fly in counter clockwise direction along a circular trajectory with radius of $r_{\mathsf{O}} = 300$ m and center at $(r_{\mathsf{O}} \cos[(n2\pi)/N], r_{\mathsf{O}} \sin[(n2\pi)/N])$. Specifically, the initial location of UAV n in time slot t can be expressed as

$$\mathbf{c}_n^0[t] = \left(r_{\mathsf{O}}\left(\cos\frac{n2\pi}{N} + \cos\frac{t2\pi}{T}\right),\ r_{\mathsf{O}}\left(\sin\frac{n2\pi}{N} + \sin\frac{t2\pi}{T}\right)\right).$$

We depict the considered users' locations and the initial trajectories of UAVs for the 2-UAV setting in Fig. 2 where the flying directions of each UAV and locations of 18 users are also shown.

In Fig. 3, we show the convergence of the MUNE and MUOE algorithms in the scenarios with 2 and 3 UAVs. It can be seen from this figure that both algorithms converge pretty fast. Moreover, the proposed MUNE algorithm achieves better performances than that of the MUOE algorithm in both scenarios. Moreover, it takes around five iterations for both algorithms to converge in the case of two UAVs, and around ten iterations in the case of three UAVs. This can be explained as follows. Larger number of UAVs in the network increases the number of variables and complexity of the optimization problems. Nevertheless, the numbers of iterations required to reach the convergence of both algorithms are sufficiently small.

We present numerical results for single-UAV and multiple-UAV settings in the following.

Numerical Results for Single-UAV Setting: We show the performances achieved by our proposed MUNE algorithm, the

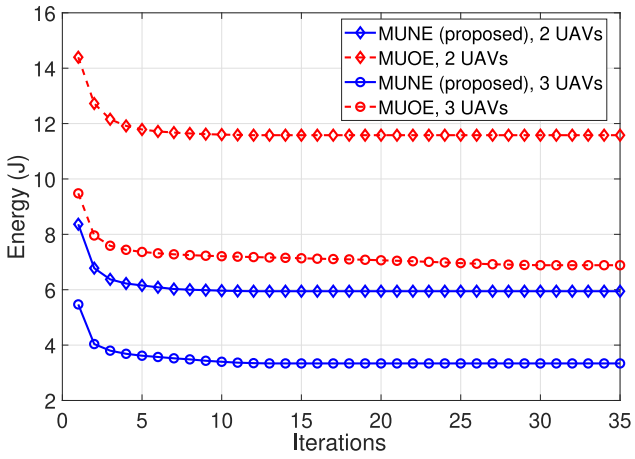

Fig. 3. Convergence of different algorithms with different numbers of UAVs.

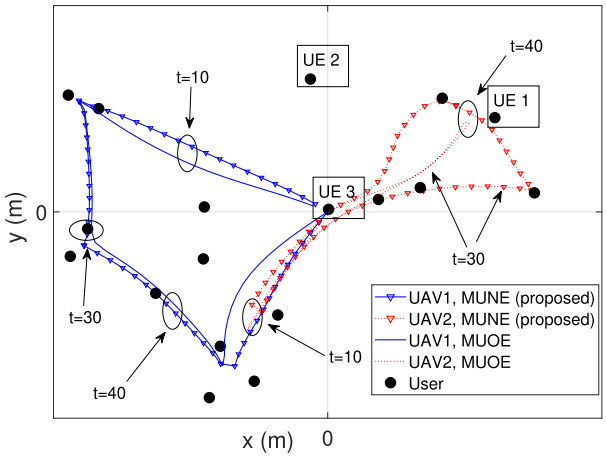

Fig. 5. UAVs' trajectories due to different algorithms.

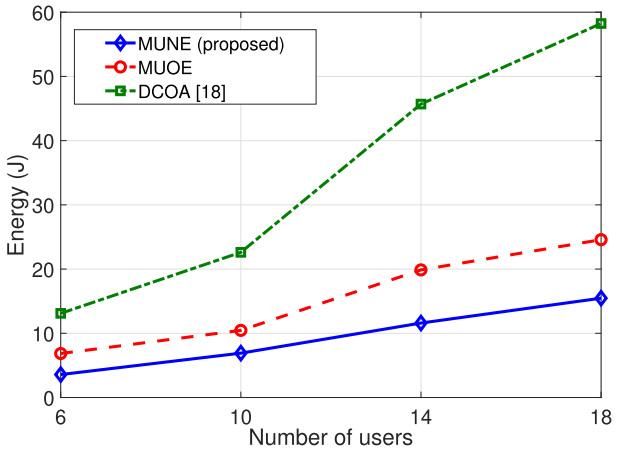

Fig. 4. Total energy consumption versus number of users for single-UAV setting.

MUOE algorithm, and the DCOA algorithm from [18] for the network setting with one UAV and varying number of users. Specifically, in Fig. 4, we show the total energy consumption of all users as these algorithms are applied. This figure shows that the proposed MUNE algorithm achieves the lowest energy consumption among the three algorithms. Moreover, the gaps between the total energy consumption due to the proposed algorithm and the two baselines increases as the number of users increases.

As for the two baselines, the MUOE algorithm still outperforms the DCOA from the energy consumption viewpoint. This can be explained by carefully analyzing the DCOA algorithm in [18] as follows. Specifically, the DCOA algorithm first attempts to reach a feasible solution by finding the user pairing and power allocation solutions with an initial UAV trajectory. Then, this algorithm employs an iterative procedure consisting of two steps in each iteration. In the first step, it determines the UAV trajectory that increases the amount of transmitted data, and then it minimizes the energy consumption with the newly obtained trajectories in the second step. Hence, the considered objective function, which is the energy consumption, is not directly optimized (in the first step), which could result in an in-efficient UAV trajectory, and hence, poor performance. For the MUOE algorithm, the objective function, after the optimal transmit power expressed as a function of other variables in (27) is substituted into it, is optimized directly. This optimization, therefore, could result in a better solution compared to that achieved by the DCOA algorithm.

Numerical Results for Multi-UAV Settings: We now present numerical results for multi-UAV settings. Note that the DCOA algorithm cannot be applied to multi-UAV settings; therefore, we only show the performance achieved by the proposed MUNE and MUOE algorithms.

We first study a particular network scenario for which users' locations and UAVs' initial trajectories are shown in Fig. 2. In Fig. 5, we show the UAVs' trajectories obtained by the MUNE and MUOE algorithms at convergence. Several interesting observations can be drawn from this figure. First, the trajectories of UAV 1 achieved by both algorithms seem to follow a convex boundary established by users located at the network edge where these edge users are closer to the initial trajectory of UAV 1 than that of UAV 2. Moreover, the trajectories of UAV 1 due to both algorithms are quite close to each other. However, there is a clear difference in the trajectories of UAV 2 obtained by the two algorithms. The trajectory obtained by the MUNE algorithm also follows the convex boundary of the edge users that are closer to the initial trajectory of UAV 2. However, the trajectory obtained by the MUOE algorithm squeezes tightly to almost a curve. This can be explained by carefully studying the users' locations. In particular, in the few time slots of the flight right after departure ($t = 0$ to $t = 10$), UAV 2 has to fly down to serve users on the bottom left-hand side of the network area. Moreover, in the second half on the flight ($t \geq 30$), this UAV has to serve users on the top right of the network area, and user 2 indicated in the figure. In order to serve a set of spatially diverged users, UAV 2 has to stay around certain desired locations that could lead to favorable channel conditions for its served users due to the nature of the OMA scheme. Specifically, OMA assigns each user a nonzero amount of bandwidth; hence, the assigned bandwidth could be wasted if the corresponding user does not transmit data. On the other hand, the NOMA scheme is more flexible and efficient in bandwidth utilization, since the total bandwidth assigned

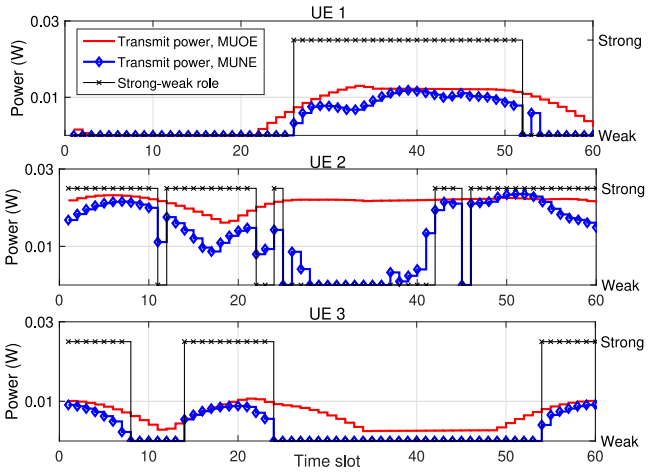

Fig. 6. Users' transmit powers over time.

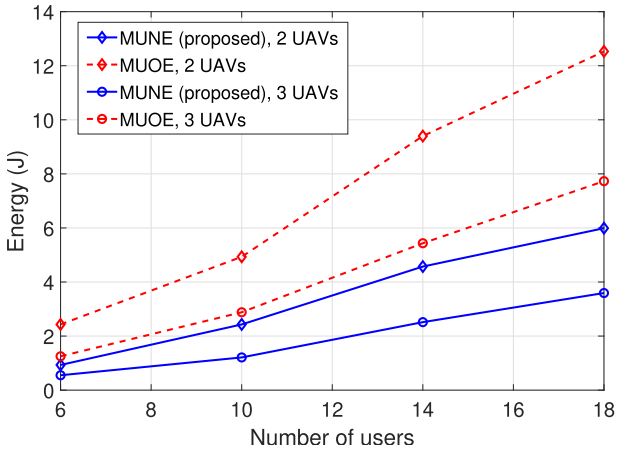

Fig. 7. Total energy versus number of users.

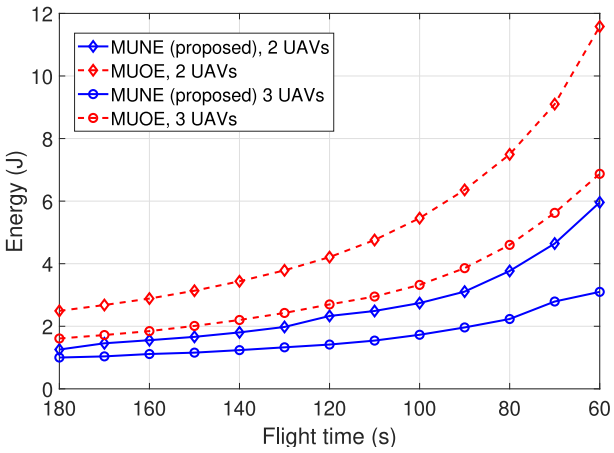

Fig. 8. Total energy versus flight time.

for a user pair can be used efficiently by both users or either one of the two paired users.

We now investigate the resource allocation solutions due to MUNE and MUOE by studying the transmit powers over time of three typical users indicated in Fig. 5: 1) (edge) user 1 that lies close to the initial trajectory of one UAV and far from the initial trajectory of the other UAV; 2) (edge) user 2 who is far away from the initial trajectories of both UAVs; and 3) (center) user 3. We plot the transmit powers over time of these three users in Fig. 6 and we also indicate their roles (strong or weak, or $\lambda_k[t] = 1$ or $\lambda_k[t] = 0$, respectively) in this figure. Note that when $p_k[t] = 0$, it does not matter if user k is assigned as a strong or weak user.[6] Therefore, if $p_k[t] = 0$, we assume that user k is a weak user for convenience.

Several interesting observations can be drawn from the figure. First, the transmit powers of users in the NOMA case are usually smaller compared to the corresponding powers due to the OMA case. Second, NOMA allows users to be inactive more frequently compared to OMA (e.g., see the transmit powers of users 2 and 3). For instance, when both UAVs are far away from user 2 (from $t = 20$ to $t = 40$), NOMA enables the user to be inactive while OMA mostly lets the user transmit with pretty high power so that user 2 can successfully transmit the required amount of data to the UAVs).

We now study the total energy due to MUNE and MUOE as different key system parameters vary. Specifically, Figs. 7 and 8 show the total energy as the number of users and the flight time (δT) vary, respectively, for network settings with 2 and 3 UAVs. It can be seen from Fig. 7 that less energy is required with more UAVs deployed in the network for both algorithms. This can be explained as follows. Each UAV tends to serve a smaller number of users in each time slot when there are more UAVs in the network. Hence, each UAV can establish a trajectory to serve a subset of users more efficiently with a larger number of UAVs. Fig. 7 again confirms that the MUNE algorithm outperforms the MUOE algorithm.

In Fig. 8, we plot the total energy versus the flight time by reducing T from $T = 180$ to $T = 60$. First, it is a bit surprising that longer flight time results in smaller energy consumption. However, the result in Fig. 8 can be explained by referring to the results in Fig. 6. In fact, both MUNE and MUOE algorithms allow a user to stay inactive when there is no UAV sufficiently close to it. Nevertheless, the proposed MUNE algorithm tends to provide more "active–inactive" cycles for individual users compared to the MUOE algorithm, as can be observed in Fig. 6. Furthermore, the results in Fig. 8 shows that the MUNE algorithm outperforms the MUOE algorithm. Finally, Fig. 8 shows us that there is a tradeoff between the total energy consumption and flight time to fulfill the demands of data collection tasks for all users. Specifically, one can decrease the flight time at the cost of higher energy consumption or one can reduce the energy consumption if the time required for the data collection can be stretched.

Fig. 9 presents the variations of total energy with required amount of transmission data D_k of each user for network settings with 2 or 3 UAVs, and $T = 60$. It can be seen from this figure that the energy consumption increases rapidly when the required amount of transmission data increases. This can be explained by noticing the logarithmic form of the achievable data rate with respect to the transmit power. However, this figure shows that as the required amount of transmission data increases, the increasing rate of the energy consumption

[6]It can be verified easily by looking at the optimal power formula (16).

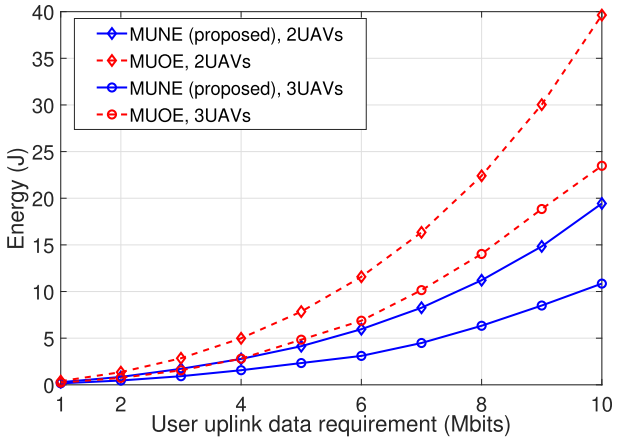

Fig. 9. Total energy versus user demand.

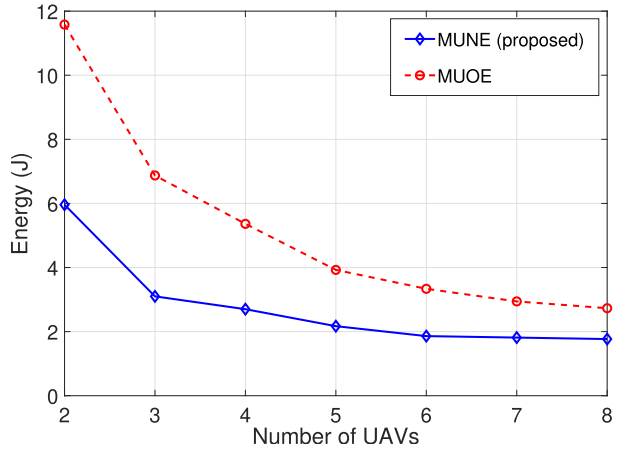

Fig. 10. Total energy versus the number of UAVs.

due to the MUNE algorithm is much lower than that due to the MUOE algorithm. This again confirms the superiority of our proposed algorithm leveraging NOMA compared to the MUOE counterpart.

Finally, we plot the energy consumption versus the number of UAVs, which varies from 2 to 8 UAVs in Fig. 10. It is expected that the energy consumption decreases when the number of UAVs increases. However, it is interesting to observe that the difference in energy consumption between the MUNE and MUOE algorithms decreases as the number of UAVs becomes larger. This implies that the gain due to NOMA over OMA is more significant in denser networks where each UAV must serve a large number of users on average. The results in this figure suggest that for network settings in which the number of users per UAV is sufficiently high (e.g., more than ten users per UAV), the employment of NOMA instead of OMA for data collection tasks in multi-UAV-based wireless networks is very rewarding.

V. Conclusion

In this article, we have tackled the energy minimization problem for the wireless networks employing multiple UAVs and NOMA where we optimize the user's transmit power, NOMA user pairing, user-UAV association, and multi-UAV trajectories. To solve the underlying MINLP problem, we first introduced a set of auxiliary variables, namely, users' data rates, and then we have derived the optimal transmit powers in terms of other variables, which are substituted into the objective function to obtain an equivalent problem. The BCD method was employed to solve the resulting problem where each set of variables (UAV trajectories, users' data rates, and integer [strong–weak and user association] variables) is optimized while the other sets of variables are given in each iteration of the algorithm. We showed that the user pairing problem can be transformed into the maximum weighted graph matching problem, which can be solved optimally in polynomial complexity. Moreover, the SCA method was employed to tackle the data rate and UAV trajectory optimization problems. Numerical studies showed that the proposed MUNE algorithm outperforms the baseline algorithms in terms of energy consumption because MUNE provides more efficient active–inactive schedules for users over the flight period compared to the MUOE algorithm. Furthermore, there is a tradeoff between the flight time and the energy consumption, i.e., longer the flight time leads to the lower energy consumption and *vice versa*.

Appendix
Multi-UAV OMA Energy Minimization Algorithm

For the benchmarking purpose, we propose a baseline algorithm in which the conventional OMA strategy instead of NOMA is employed. The baseline is named the MUOE *Algorithm*. We describe MUOE in details in this Appendix. Let $p_k[t]$ be the transmit power that user k uses to transmit data to its associated UAV in time slot t. The optimization problem for this OMA-based strategy can be formulated as follows:

$$\mathcal{P}_0^{\mathsf{OMA}}: \min_{\{\mathbf{p}[t],\mathbf{c}_n[t]\}} \delta \sum_{t=1}^{T}\sum_{k=1}^{K} p_k[t]$$

$$\text{s.t. } \delta \sum_{t=1}^{T} \frac{B}{2}\log\left(1+\frac{\tau_k[t]p_k[t]}{\sigma^2/2}\right) \geq D_k \quad \forall k,t \tag{26a}$$

$$p_k[t] \leq P_{\max} \quad \forall k,t \tag{26b}$$

$$\text{constraints} \quad (11e), (11f), (11g).$$

It can be verified that problem $\mathcal{P}_0^{\mathsf{OMA}}$ is nonconvex. Moreover, the appearance of the transmit power variables in the objective function prevents us from applying the BCD method to solve the problem. We employ a similar method, which was used to develop our NOMA-based algorithm, to tackle problem $\mathcal{P}_0^{\mathsf{OMA}}$. Specifically, we first introduce the auxiliary variables $\{\mathbf{r}[t]\}$ where $r_k[t]$ is the data rate that user k transmits data to its associated UAV in time slot t. Let $\{\mathbf{p}^*[t]\}$ be the optimal power allocation of $\mathcal{P}_0^{\mathsf{OMA}}$, then

$$p_k^*[t] = \frac{\sigma^2}{2}\tau_k^{-1}[t]\left(2^{2r_k[t]/B}-1\right). \tag{27}$$

The derivation of (27) is similar to that of the NOMA case presented in Lemma 1, and is omitted here. Substituting the right-hand side of (27) into the objective function of $\mathcal{P}_0^{\mathsf{OMA}}$,

we can obtain an equivalent optimization problem of $\mathcal{P}_0^{\mathsf{OMA}}$, which can be solved by using the BCD approach. Specifically, $\{\mathbf{r}[t]\}$ and $\{\mathbf{c}_n[t]\}$ are optimized iteratively until convergence. The optimization problem when one optimizes $\{\mathbf{r}[t]\}$ given $\{\mathbf{c}_n[t]\}$ can be expressed as

$$\mathcal{P}_{\mathsf{R}}^{\mathsf{OMA}}: \min_{\{\mathbf{r}[t]\}} \delta \frac{\sigma^2}{2} \sum_{t=1}^{T} \sum_{k=1}^{K} \tau_k^{-1}[t]\left(2^{2r_k[t]/B} - 1\right)$$

$$\text{s.t. } \delta \sum_{t=1}^{T} r_k[t] \geq D_k \quad \forall k, \tag{28a}$$

$$\frac{\sigma^2}{2} \tau_k^{-1}[t]\left(2^{2r_k[t]/B} - 1\right) \leq P_{\max} \quad \forall k, t. \tag{28b}$$

Problem $\mathcal{P}_{\mathsf{R}}^{\mathsf{OMA}}$ is convex because it has a convex objective function and convex constraints. Hence, it can be solved efficiently by using the CVX solver.

Let $\mathbf{c}_{(k)}[t]$ be the coordinate of the UAV serving user k in time slot t. Note that $\tau_k^{-1}[t] = \mu^{-1}(\|\mathbf{c}_{(k)}[t] - \mathbf{u}_k\|^2 + h^2)$, the UAV trajectory optimization problem, given $\{\mathbf{r}[t]\}$, can be expressed as follows:

$$\mathcal{P}_{\mathsf{C}}^{\mathsf{OMA}}: \min_{\{\mathbf{c}_n[t]\}} \delta \sum_{t=1}^{T} \sum_{k=1}^{K} \eta_k[t]\left(\left\|\mathbf{c}_{(k)}[t] - \mathbf{u}_k\right\|^2 + h^2\right)$$

$$\text{s.t. } \eta_k[t]\left(\left\|\mathbf{c}_{(k)}[t] - \mathbf{u}_k\right\|^2 + h^2\right) \leq P_{\max} \quad \forall k, t$$

$$\text{constraints (11e), (11f), (11g)} \tag{29a}$$

where $\eta_k[t] = (\sigma^2/2\mu)(2^{2r_k[t]/B} - 1)$.

It can be verified that problem $\mathcal{P}_{\mathsf{C}}^{\mathsf{OMA}}$ is still nonconvex. However, it can be solved by using the SCA technique where constraint (11f) is approximated by constraint (25) as in the development of our MUNE algorithm.

In summary, we can solve problem $\mathcal{P}_0^{\mathsf{OMA}}$ by using the BCD technique to tackle the transformed problem where problems $\mathcal{P}_{\mathsf{R}}^{\mathsf{OMA}}$ and $\mathcal{P}_{\mathsf{C}}^{\mathsf{OMA}}$ are solved iteratively until convergence. This iterative algorithm is refereed to as the MUOE algorithm.

REFERENCES

[1] A. Fotouhi *et al.*, "Survey on UAV cellular communications: Practical aspects, standardization advancements, regulation, and security challenges," *IEEE Commun. Surveys Tuts.*, vol. 21, no. 4, pp. 3417–3442, 4th Quart., 2019.

[2] "LTE Unmanned Aircraft Systems." Qualcomm Technologies. May 2017. Accessed: Mar. 20, 2021. [Online]. Available: https://www.qualcomm.com/media/documents/files/lte-unmanned-aircraft-systems-trial-report.pdf

[3] N. H. Motlagh, T. Taleb, and O. Arouk, "Low-altitude unmanned aerial vehicles-based Internet of Things services: Comprehensive survey and future perspectives," *IEEE Internet Things J.*, vol. 3, no. 6, pp. 899–922, Dec. 2016.

[4] S. Sekander, H. Tabassum, and E. Hossain, "Multi-tier drone architecture for 5G/B5G cellular networks: Challenges, trends, and prospects," *IEEE Commun. Mag.*, vol. 56, no. 3, pp. 96–103, Mar. 2018.

[5] "Cisco Annual Internet Report." Cisco. Mar. 2020. Accessed: Sep. 20, 2021. [Online]. Available: https://www.cisco.com/c/en/us/solutions/collateral/executive-perspectives/annual-internet-report/white-paper-c11-741490.pdf

[6] N. C. Luong, D. T. Hoang, P. Wang, D. Niyato, D. I. Kim, and Z. Han, "Data collection and wireless communication in Internet of Things (IoT) using economic analysis and pricing models: A survey," *IEEE Commun. Surveys Tuts.*, vol. 18, no. 4, pp. 2546–2590, 4th Quart., 2016.

[7] C. Zhan, Y. Zeng, and R. Zhang, "Energy-efficient data collection in UAV enabled wireless sensor network," *IEEE Wireless Commun. Lett*, vol. 7, no. 3, pp. 328–331, Jun. 2018.

[8] J. Gong, T.-H. Chang, C. Shen, and X. Chen, "Flight time minimization of UAV for data collection over wireless sensor networks," *IEEE J. Sel. Areas Commun.*, vol. 36, no. 9, pp. 1942–1954, Sep. 2018.

[9] W. Wang, N. Zhao, L. Chen, X. Liu, Y. Chen, and D. Niyato, "UAV-assisted time-efficient data collection via uplink NOMA," *IEEE Trans. Commun.*, vol. 69, no. 11, pp. 7851–7863, Nov. 2021.

[10] Y. Saito, Y. Kishiyama, A. Benjebbour, T. Nakamura, A. Li, and K. Higuchi, "Non-orthogonal multiple access (NOMA) for cellular future radio access," in *Proc. IEEE VTC-Spring*, 2013, pp. 1–5.

[11] R. Duan, J. Wang, C. Jiang, H. Yao, Y. Ren, and Y. Qian, "Resource allocation for multi-UAV aided IoT NOMA uplink transmission systems," *IEEE Internet Things J.*, vol. 6, no. 4, pp. 7025–7037, Aug. 2019.

[12] R. Zhang, X. Pang, J. Tang, Y. Chen, N. Zhao, and X. Wang, "Joint location and transmit power optimization for NOMA-UAV networks via updating decoding order," *IEEE Wireless Commun. Lett*, vol. 10, no. 1, pp. 136–140, Jan. 2021.

[13] F. Cui, Y. Cai, Z. Qin, M. Zhao, and G. Y. Li, "Multiple access for mobile-UAV enabled networks: Joint trajectory design and resource allocation," *IEEE Trans. Commun.*, vol. 67, no. 7, pp. 4980–4994, Jul. 2019.

[14] L. Lei, D. Yuan, and P. Värbrand, "On power minimization for non-orthogonal multiple access (NOMA)," *IEEE Commun. Lett.*, vol. 20, no. 12, pp. 2458–2461, Dec. 2016.

[15] X. Li, C. Li, and Y. Jin, "Dynamic resource allocation for transmit power minimization in OFDM-based NOMA systems," *IEEE Commun. Lett.*, vol. 20, no. 12, pp. 2558–2561, Dec. 2016.

[16] M. Zeng, A. Yadav, O. A. Dobre, and H. V. Poor, "Energy-efficient joint user-RB association and power allocation for uplink hybrid NOMA-OMA," *IEEE Internet Things J.*, vol. 6, no. 3, pp. 5119–5131, Jun. 2019.

[17] Z. Chen, Z. Ding, X. Dai, and R. Zhang, "An optimization perspective of the superiority of NOMA compared to conventional OMA," *IEEE Trans. Signal Process.*, vol. 65, no. 19, pp. 5191–5202, Oct. 2017.

[18] J. Zhao, Y. Wang, Z. Fei, X. Wang, and Z. Miao, "NOMA-aided UAV data collection system: Trajectory optimization and communication design," *IEEE Access*, vol. 8, pp. 155843–155858, 2020.

[19] W. Shi *et al.*, "Joint UL/DL resource allocation for UAV-aided full-duplex NOMA communications," *IEEE Trans. Commun*, vol. 69, no. 12, pp. 8474–8487, Dec. 2021.

[20] X. Zhang, J. Zhang, J. Xiong, L. Zhou, and J. Wei, "Energy-efficient multi-UAV-enabled multiaccess edge computing incorporating NOMA," *IEEE Internet Things J.*, vol. 7, no. 6, pp. 5613–5627, Jun. 2020.

[21] Y. Liu, Z. Qin, M. Elkashlan, Z. Ding, A. Nallanathan, and L. Hanzo, "Nonorthogonal multiple access for 5G and beyond," *Proc. IEEE*, vol. 105, no. 12, pp. 2347–2381, Dec. 2017.

[22] J. Wang *et al.*, "Multiple unmanned-aerial-vehicles deployment and user pairing for nonorthogonal multiple access schemes," *IEEE Internet Things J.*, vol. 8, no. 3, pp. 1883–1895, Feb. 2021.

[23] W. Chen, S. Zhao, R. Zhang, Y. Chen, and L. Yang, "UAV-assisted data collection with nonorthogonal multiple access," *IEEE Internet Things J.*, vol. 8, no. 1, pp. 501–511, Jan. 2021.

[24] J. Lu *et al.*, "UAV-enabled uplink non-orthogonal multiple access system: Joint deployment and power control," *IEEE Trans. Veh. Technol.*, vol. 69, no. 9, pp. 10090–10102, Sep. 2020.

[25] X. Liu *et al.*, "Placement and power allocation for NOMA-UAV networks," *IEEE Wireless Commun. Lett*, vol. 8, no. 3, pp. 965–968, Jun. 2019.

[26] M. T. Nguyen and L. B. Le, "NOMA user pairing and UAV placement in UAV-based wireless networks," in *Proc. IEEE ICC*, 2019, pp. 1–6.

[27] X. Mu, Y. Liu, L. Guo, J. Lin, and Z. Ding, "Energy-constrained UAV data collection systems: NOMA and OMA," *IEEE Trans. Veh. Technol.*, vol. 70, no. 7, pp. 6898–6912, Jul. 2021.

[28] N. Zhao *et al.*, "Joint trajectory and precoding optimization for UAV-assisted NOMA networks," *IEEE Trans. Commun.*, vol. 67, no. 5, pp. 3723–3735, May 2019.

[29] H. Zhang, J. Zhang, and K. Long, "Energy efficiency optimization for NOMA UAV network with imperfect CSI," *IEEE J. Sel. Areas Commun.*, vol. 38, no. 12, pp. 2798–2809, Dec. 2020.

[30] J. Edmonds, "Paths, trees, and flowers," *Can. J. Math.*, vol. 17, pp. 449–467, Nov. 2018.

[31] "Study on enhanced LTE support for aerial vehicles," 3GPP, Sophia Antipolis, France, Rep. 3GPP-TR-36.777, 2017. Accessed: Sep. 13, 2021. [Online]. Available: http://www.3gpp.org/dynareport/36777.htm

[32] Y. Liu, Z. Qin, Y. Cai, Y. Gao, G. Y. Li, and A. Nallanathan, "UAV communications based on non-orthogonal multiple access," *IEEE Wireless Commun.*, vol. 26, no. 1, pp. 52–57, Feb. 2019.

[33] S. Boyd and L. Vandenberghe, *Convex Optimization*. Cambridge, U.K.: Cambridge Univ. Press, 2004.

[34] Z. Galil, S. Micali, and H. Gabow, "An O(EV\logV) algorithm for finding a maximal weighted matching in general graphs," *SIAM J. Comput.*, vol. 15, no. 1, pp. 120–130, 1986.
[35] R. Duan and S. Pettie, "Linear-time approximation for maximum weight matching," *J. ACM*, vol. 61, no. 1, pp. 1–23, 2014.
[36] Y. Fu, Y. Zhang, Q. Zhu, M. Chen, and T. Q. S. Quek, "Joint content caching, recommendation, and transmission optimization for next generation multiple access networks," *IEEE J. Sel. Areas Commun.*, vol. 40, no. 5, pp. 1600–1614, May 2022.
[37] Y. Nesterov and A. Nemirovskii, *Interior-Point Polynomial Algorithms in Convex Programming*. Philadelphia, PA, USA: SIAM, 1994.
[38] A. M. Geoffrion, "Generalized benders decomposition," *J. Optim. Theory Appl.*, vol. 10, no. 4, pp. 237–260, 1972.

Minh Tri Nguyen (Student Member, IEEE) received the B.Eng. and M.Eng. degrees in electrical engineering from International University, Ho Chi Minh National University, Ho Chi Minh City, Vietnam, in 2014 and 2016, respectively, and the Ph.D. degree in telecommunications from the Institut National de la Recherche Scientifique, University of Quebec, Montreal, QC, Canada, in 2022.

His current research interests include interference mitigation, radio resource management, 5G new radio, and aerial-based communications for 5G and beyond 5G networks.

Long Bao Le (Senior Member, IEEE) received the B.Eng. degree in electrical engineering from Ho Chi Minh City University of Technology, Ho Chi Minh City, Vietnam, in 1999, the M.Eng. degree in telecommunications from Asian Institute of Technology, Khlong Nueng, Thailand, in 2002, and the Ph.D. degree in electrical engineering from the University of Manitoba, Winnipeg, MB, Canada, in 2007.

He was a Postdoctoral Researcher with Massachusetts Institute of Technology, Cambridge, MA, USA, from 2008 to 2010, and University of Waterloo, Waterloo, ON, Canada, from 2007 to 2008. Since 2010, he has been with the Institut National de la Recherche Scientifique, University of Quebec, Montreal, QC, Canada, where he is currently a full professor. His current research interests include smartgrids, radio resource management, network control and optimization, and emerging enabling technologies for 5G wireless and beyond systems. He is the Coauthor of the books *Radio Resource Management in Multi-Tier Cellular Wireless Networks* (Wiley, 2013) and *Radio Resource Management in Wireless Networks: An Engineering Approach* (Cambridge University Press, 2017).

Dr. Le was a member of the editorial board of IEEE TRANSACTIONS ON WIRELESS COMMUNICATIONS and IEEE COMMUNICATIONS SURVEYS AND TUTORIALS.